



## Future change in Southern Hemisphere summertime and wintertime atmospheric blockings simulated using a 20-km-mesh AGCM

Mio Matsueda,<sup>1,2</sup> Hirokazu Endo,<sup>2</sup> and Ryo Mizuta<sup>2</sup>

Received 12 November 2009; revised 11 December 2009; accepted 23 December 2009; published 22 January 2010.

[1] Future changes in the frequency of Australia–New Zealand (AU; winter and summer) and Andes (AN; winter) blockings are investigated via present-day (1979–2003) and future (2075–2099) simulations using 20-, 60-, and 180-km-mesh atmospheric general circulation models (AGCMs) under the IPCC SRES A1B emission scenario. The present-day climate simulations reveal that the AGCM with the highest horizontal resolution is required to accurately simulate AU and AN blockings in both winter and summer. The future climate simulation predicts a significant decrease in AU blocking frequency in both summer and winter, mainly on the west side of the peak in present-day blocking frequency, where the westerly jet is predicted to increase in strength. The decrease in the AU blocking frequency during winter is more remarkable than that during summer. The number of long-lived AU blocking events is predicted to decrease with the possibility that events  $\geq 13$  days will disappear altogether. In contrast, no significant changes are predicted in AN blocking frequency and duration. **Citation:** Matsueda, M., H. Endo, and R. Mizuta (2010), Future change in Southern Hemisphere summertime and wintertime atmospheric blockings simulated using a 20-km-mesh AGCM, *Geophys. Res. Lett.*, 37, L02803, doi:10.1029/2009GL041758.

### 1. Introduction

[2] Atmospheric blocking can persist for a long time, leading to extremely high or low temperatures and severe precipitation anomalies over the surrounding area. Many studies have investigated extreme weather events related to blocking, the mechanism of blocking, and model performance in simulating blocking [e.g., Mendes *et al.*, 2008; Trigo *et al.*, 2004; Cash and Lee, 2000; D'Andrea *et al.*, 1998; Trenberth and Mo, 1985].

[3] It is well known that general circulation models tend to underestimate blocking frequency [Palmer *et al.*, 2008; D'Andrea *et al.*, 1998; Tibaldi *et al.*, 1994], thereby making it difficult to reliably determine future changes in atmospheric blocking. In fact, future change in blocking was not commented upon in the IPCC-AR4 report [Intergovernmental Panel on Climate Change, 2007], even though it is important to estimate the frequency of blocking in the future climate.

[4] Matsueda *et al.* [2009] investigated the future change in Northern Hemisphere wintertime blocking based on simulations using a 20-km-mesh atmospheric global circulation model (AGCM; TL959L60), which performs well in simulating blocking in the present climate simulation. The

authors reported that the frequencies of wintertime Euro-Atlantic and Pacific blockings are predicted to show a significant decrease, mainly on the west side of the peak in present-day blocking frequency, where the westerlies are predicted to increase in strength; no significant change was predicted on the east side of the peak. The authors also raised the possibility that long-lived ( $>25$  days) Euro-Atlantic and Pacific blockings will disappear altogether in the future.

[5] In the present study, we focus on the frequency and duration of Australia–New Zealand and Andes blockings simulated using the TL959L60, TL319L60 (60 km), and TL95L40 (180 km) models for the Southern Hemisphere winter (June–August (JJA)) and summer (December–February (DJF)) in the present-day (1979–2003) and future (2075–2099) climates. For the present-day climate, we mainly compare the frequency of simulated blocking with observed data and evaluate the influence of the horizontal resolution of the AGCM on model performance in simulating blocking events. For the future climate, we consider future changes in blocking frequency and duration based on the model's ability to simulate blocking in the present-day climate. To estimate the degree of uncertainty in future projections of blocking, we conducted initial-value ensemble simulations using the 60-km-mesh AGCM.

### 2. Methodology

#### 2.1. Model Experiments

[6] The experimental settings employed in this study are the same as those used by Matsueda *et al.* [2009]; consequently, only a brief description is given here. The employed AGCM was developed by the Meteorological Research Institute (MRI), Japan, for performing long-term climate simulations, and is based on the operational medium-range numerical weather prediction model developed by the Japan Meteorological Agency (JMA) [Mizuta *et al.*, 2006]. Model integrations were conducted with three different horizontal resolutions for the present-day (1979–2003) and future (2075–2099) climates: TL959L60 (horizontal grid size of 20 km), TL319L60 (60 km), and TL95L40 (180 km), where the number following TL indicates the total wavenumber in a triangular spectral truncation based on a Gaussian grid, and the number following L indicates the number of vertical levels. To estimate the uncertainty involved in future projections of blocking, an initial-value ensemble simulation was performed using the TL319L60 AGCM for the present-day and future climates, with three arbitrary initial values.

[7] For the present-day simulation, the AGCM was integrated using observed historical sea surface temperature (SST). For the future simulation, the SST climate-change signals were estimated using the CMIP3 multi-model ensemble mean to which detrended interannual variations

<sup>1</sup>AESTO, MRI, Tsukuba, Japan.

<sup>2</sup>Climate Research Department, MRI, Tsukuba, Japan.

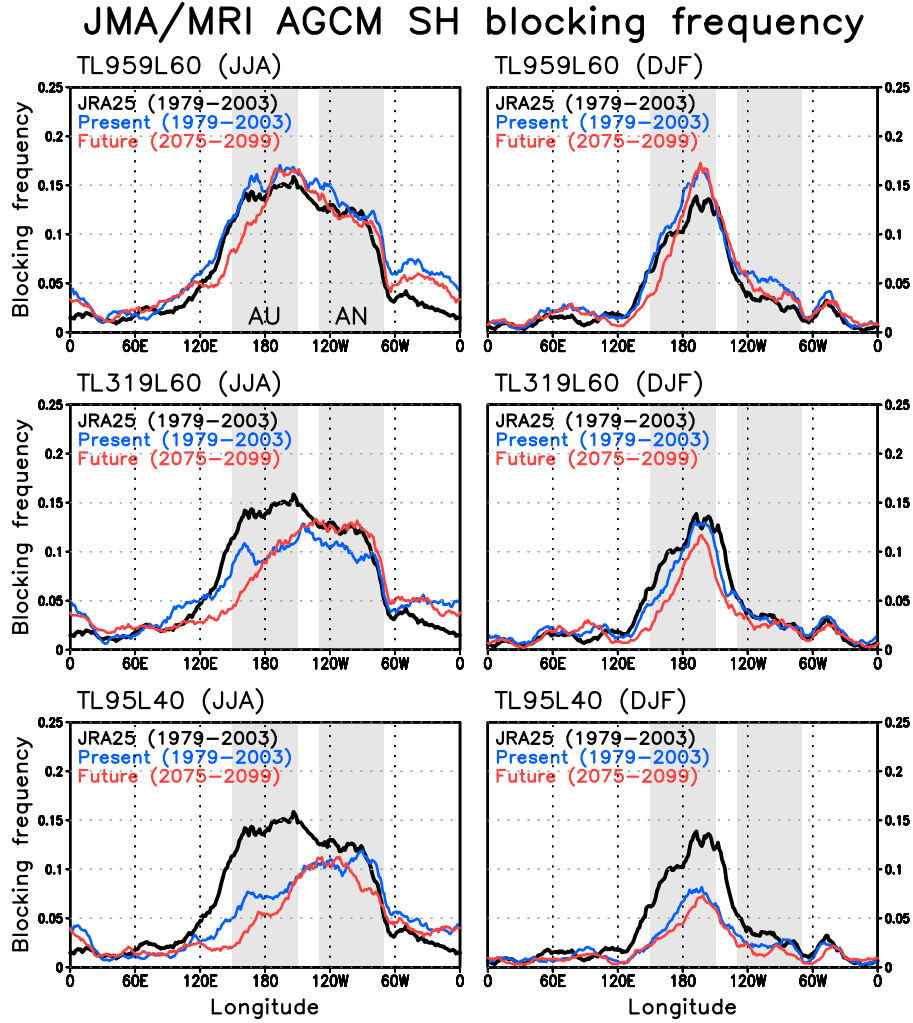


**Figure 1.** Frequency of Southern Hemisphere (SH) (left) wintertime (June to August) and (right) summertime (December to February) blockings as a function of longitude for the (top) TL959L60, (middle row) TL319L60, and (bottom) TL95L40 AGCMs. The black, blue, and red lines represent JRA25, present-day, and future simulations, respectively.

in HadISST had been added [Mizuta *et al.*, 2008]. The IPCC SRES A1B scenario was assumed for future emissions of greenhouse gases.

## 2.2. Blocking Index

[8] The data used in this study consist of the daily 500 hPa geopotential height (Z500) field at 1200 UTC observed and produced by the long-term integration of the AGCM. The Japanese reanalysis (JRA25) [Onogi *et al.*, 2007] was adopted as the observation data for the period 1979–2003. Before calculation of the blocking index, the data were interpolated to a grid spacing of 1.25°.

[9] We used an objective blocking index based on *Tibaldi et al.* [1994]; only a brief definition is given here. The 500 hPa Geopotential Height meridional Gradients, GHGS (South) and GHGN (North), are computed for each latitude as follows:

$$\begin{cases} \text{GHGS} = \frac{Z(\phi_s) - Z(\phi_0)}{\phi_s - \phi_0}, \\ \text{GHGN} = \frac{Z(\phi_0) - Z(\phi_n)}{\phi_0 - \phi_n}, \end{cases} \quad (1)$$

where

$$\begin{cases} \phi_n = 35.0^\circ\text{S} \pm \Delta, \\ \phi_0 = 50.0^\circ\text{S} \pm \Delta, \\ \phi_s = 65.0^\circ\text{S} \pm \Delta, \end{cases} \\ \Delta = 0^\circ, 1.25^\circ, 2.5^\circ, 3.75^\circ, 5.0^\circ.$$

[10] A specific longitude on a given day is defined as being blocked if both of the following conditions are satisfied (for at least one value of  $\Delta$ ):

$$\begin{cases} \text{GHGS} < -5\text{m/deg lat}, \\ \text{GHGN} > 0. \end{cases} \quad (2)$$

[11] Similarly to *Tibaldi et al.* [1994], the two main sectors of the Southern Hemisphere that are particularly prone to blocking are defined using the following longitudinal limits: Australia–New Zealand (AU), 150°E–150°W; Andes (AN), 130°W–70°W. A sector is then defined as being blocked if three or more adjacent longitudes within its limits are blocked according to the previous local and

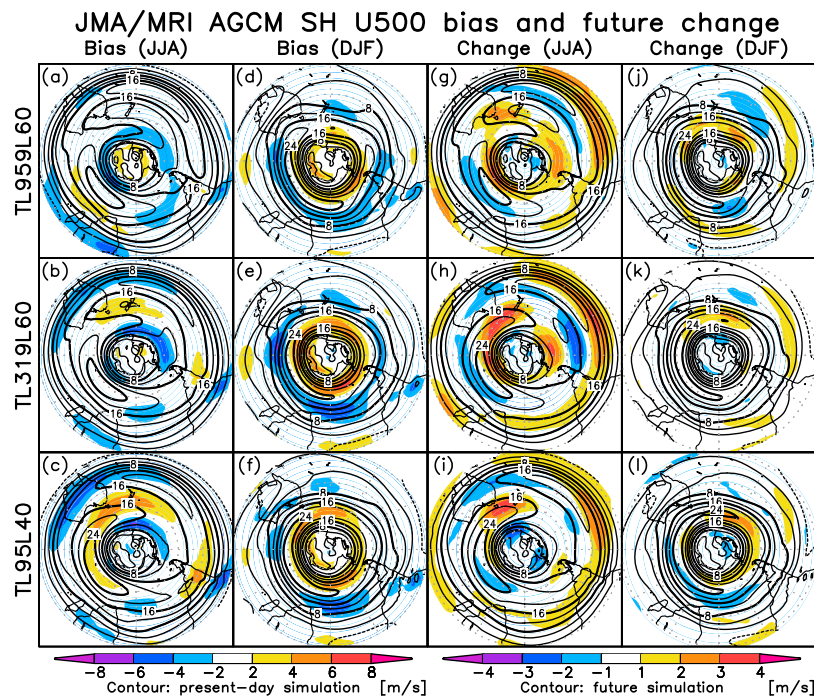


**Figure 2.** (a)–(f) Present-day 500-hPa horizontal wind (U500) (contour) and bias in U500 against JRA25 (1979–2003) (shaded) and (g)–(l) future U500 (contour) and future change in U500 (2075–2099) (shaded) for the (top) TL959L60, (middle) TL319L60, and (bottom) TL95L40 AGCMs.

instantaneous index definition (“sector blocking”). Blocking duration is calculated for sector blocking.

### 3. Results

#### 3.1. Present-Day Climate Experiments

[12] Figure 1 shows the blocking frequency as a function of longitude for JRA25 (black lines) and AGCMs (blue lines) in the present-day climate. In the Southern Hemisphere, the observed blocking frequency shows blocking maxima in the AU and AN sectors during winter (JJA) and in the AU sector during summer (DJF). It is well known that general circulation models tend to underestimate blocking frequency [Palmer *et al.*, 2008; D’Andrea *et al.*, 1998; Tibaldi *et al.*, 1994]. TL959L60 is in good agreement with JRA25 with respect to the frequencies of AU and AN blockings in JJA and DJF, although TL959L60 shows slight overestimations. The higher the horizontal resolution is, the more accurate the simulated blocking frequency is, as in the wintertime Euro-Atlantic blocking case described by Matsueda *et al.* [2009]. TL959L60 has smaller biases in Z500 (not shown) and 500 hPa horizontal wind (U500) climatologies over the AU and AN sectors in JJA and DJF than do the lower-resolution models (Figures 2a–2f). In the Southern Hemisphere winter, it is well known that the climatological westerlies have a spiral pattern of wind maxima, starting around Australia at about 30°S, surrounding Antarctica, and ending around the central southern Pacific at about 60°S [Trenberth, 1979]. Wintertime AU blocking is known to be characterized by a split in the mean westerlies over New Zealand [Trenberth and Mo, 1985]. The split jet is composed of the subtropical jet on its equatorward branch and the polar front jet (PFJ) on its poleward branch [Bals-Elsholz *et al.*, 2001]. In the lower-

resolution models, positive westerlies biases over the split due to an equatorward shift of the PFJ suggesting less meandering and diffluent flows correspond to the reduced frequency of AU blocking (Figures 2b–2c).

[13] Figure 3 shows the ensemble-mean blocking frequency obtained in the ensemble simulation using TL319L60 in the present-day climate (blue lines). The standard deviation of blocking frequency measured by ensemble members (range of blue shaded area) is small compared with the ensemble mean of blocking frequencies (blue solid line) in present-day climate. The range in blocking frequency during JJA tends to be larger than that during DJF.

[14] Figure 4 shows the AU blocking duration for JRA25 (white diamonds) and AGCMs (green bars) in JJA and DJF in the present-day climate. The present-day distribution of AU blocking duration simulated by TL959L60 is in good agreement with JRA25 in both JJA and DJF (Figures 4a–4b), whereas the TL319L60 ensemble simulation tends to underestimate the mean number of AU blockings of almost all durations (Figures 4c–4d), especially in the long-lived ( $\geq 12$  days) wintertime AU blockings. TL959L60 performs well in simulating long-lived AU blockings, as in the wintertime Euro-Atlantic blocking case reported by Matsueda *et al.* [2009]. In both JJA and DJF, TL95L40 underestimates the number of AU blockings to a greater degree than does TL319L60, particularly in the case of long-lived blockings (not shown). For both TL319L60 and TL95L40, the positive westerlies biases over the split may suggest a difficulty in simulating long-lived AU blockings.

#### 3.2. Future Climate Experiments

[15] For JJA of the future, all the models show a decrease in AU blocking frequency on the west side of the peak in present-day blocking frequency (Figure 1, left), as in the

## JMA/MRI AGCM SH blocking frequency (TL319L60)

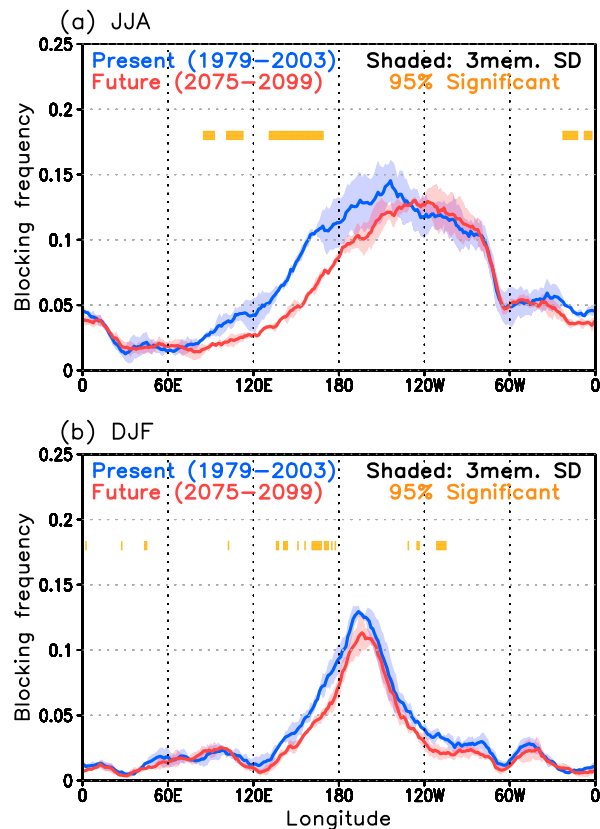


**Figure 3.** Future change and its uncertainty in the frequency of Southern Hemisphere (a) wintertime (June to August) and (b) summertime (December to February) blocking estimated by the TL319L60 AGCM (60 km) ensemble simulation. Blue and red lines represent three-member initial-value ensemble means of the blocking frequency in the present-day and future simulations, respectively. Blue and red shaded areas represent the  $\pm 1$  standard deviation of the blocking frequency measured from the ensemble members. Orange bars indicate the longitudes for which the future change in the blocking frequency is significant at the 0.05 level of confidence.

Northern Hemisphere wintertime blocking case reported by Matsueda *et al.* [2009]. The ensemble simulation by TL319L60 predicts a decrease in the frequency of AU blocking on the west side of the peak, statistically significant at the 0.05 level of confidence (Figure 3a). TL959L60 predicts that long-lived ( $\geq 13$  days) AU blockings will disappear in the future climate and that short-lived ( $\leq 9$  days) AU blockings will occur more frequently (Figure 4a). The disappearance of long-lived blockings has also been predicted for Northern Hemisphere wintertime blocking [Matsueda *et al.*, 2009]. Compared with the present-day simulation by TL319L60, that in the future climate tends to predict a smaller number of AU blockings of almost all durations (Figure 4c). The decrease in AU blocking frequency and the disappearance of long-lived AU blocking might be related to an intensification of the westerlies over the split due to an equatorward shift of the PFJ from south of Australia to south of New Zealand (shaded areas in Figures 2g–2i). Archer

and Caldeira [2008] also showed an observed fact of the equatorward shift of the PFJ using reanalysis datasets. The split over New Zealand is less remarkable in the future than in the present, especially in TL319L60 and TL95L40 (contours in Figures 2h–2i). The split in TL959L60 shifts eastward in the future with intensification of the westerlies.

[16] In terms of the AN blocking frequency in JJA of the future, TL319L60 shows an increase in frequency, whereas TL959L60 and TL95L40 show a decrease (Figure 1, left). The TL319L60 ensemble simulation, however, predicts no significant change in AN blocking frequency (Figure 3a). The future AN blocking frequency will be similar to the present one. No remarkable changes are predicted in AN blocking duration (not shown).

[17] In DJF of the future, TL959L60 and TL95L40 predict decreased frequencies of AU blocking on the west side of the peak in present-day blocking frequency (Figure 1, right). Although TL319L60 predicts a uniform decrease in AU blocking frequency between  $150^{\circ}\text{E}$  and  $150^{\circ}\text{W}$ , the ensemble simulation by TL319L60 shows a significant decrease in AU blocking frequency on the west side of the peak in present-day mean blocking frequency (Figure 3b). The magnitude of the decrease in AU blocking frequency during DJF is smaller than that during JJA. The decrease in AU blocking frequency is consistent with the stronger westerlies south of New Zealand in the future climate (Figures 2j–2l), as seen in the case in JJA. In terms of blocking duration, TL959L60 predicts a slight decrease in the frequency of long-lived ( $\geq 8$  days) AU blockings in the future climates (Figure 4b). The ensemble simulation by TL319L60 also predicts a slight decrease in the number of long-lived ( $\geq 7$  days) AU blockings in the future climate (Figure 4d).

#### 4. Summary and Conclusion

[18] We investigated future changes in the frequency of Australia–New Zealand (AU; winter and summer) and Andes (AN; winter) blockings via present-day (1979–2003) and future (2075–2099) simulations using 20-, 60-, and 180-km-mesh AGCMs under the IPCC SRES A1B emission scenario. The results of present-day climate simulations reveal that the AGCM with the highest horizontal resolution is required to accurately simulate AU and AN blockings for both winter and summer. The 20-km-mesh AGCM performs well in simulating long-lived wintertime AU blockings, whereas the lower-resolution models underestimate the number of long-lived AU blockings. Wintertime AU blocking is known to be characterized by a split in the mean westerlies over New Zealand. The lower-resolution models show positive westerlies biases due to an equatorward shift of the polar front jet (PFJ) in the present-day winter; i.e., they simulate a less remarkable split over New Zealand and the less frequency in AU blocking. The Rossby wave train from southern Indian Ocean is important for formation of the split over New Zealand [Inatsu and Hoskins, 2004]. The simulated indistinct Rossby wave train from southern Indian Ocean in the lower-resolution models (not shown) might result in the positive westerlies biases and the lack of longer-lived AU blockings.

[19] In winter and summer of the future, significant decreases in AU blocking frequency are predicted. It is

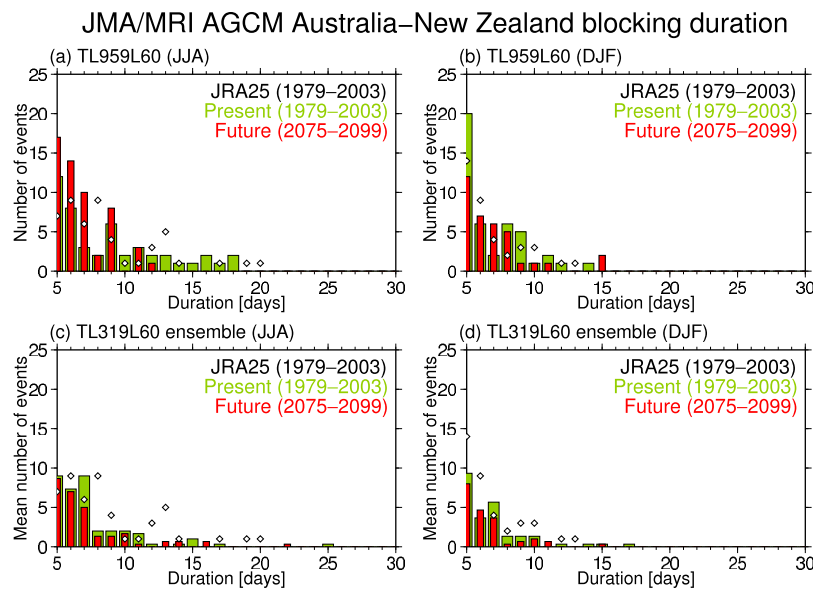


**Figure 4.** Duration of (left) wintertime (June to August) and (right) summertime (December to February) Australia–New Zealand (AU) blockings simulated using the (top) TL959L60 and (bottom) TL319L60 AGCMs. White diamonds represent JRA25. Green and red bars represent the number of AU blocking events in the present-day and future simulations, respectively. Results obtained from the TL319L60 AGCM represent the mean of the three initial-value ensemble members.

interesting that the decreases of blocking frequency in future Northern and Southern Hemisphere are seen on the west side of the peak in the present-day blocking frequency. In summer, the Southern Annular Mode (SAM) during summer dictates the strength of the mid-latitude westerlies at most longitudes. The decrease in AU blocking frequency during summer might be due to an increase in the SAM reported by *Intergovernmental Panel on Climate Change* [2007]. The decrease in AU blocking frequency during winter is more remarkable than that during summer. In winter, the decrease in AU blocking frequency is related to the equatorward shift of the PFJ. *Inatsu and Hoskins* [2004] showed that an experiment with zonally symmetric tropical sea surface temperatures (SSTs) destroys the spiral structure of the westerlies in the Southern Hemisphere through a change in Rossby wave train from southern Indian Ocean. A reason of the decrease in AU blocking frequency might result from a fact that the zonal gradient of the tropical SSTs tends to decrease under the global warming [*Intergovernmental Panel on Climate Change*, 2007]. The number of long-lived AU blocking events is predicted to decrease, with the possibility that long-lived ( $\geq 13$  days) AU blocking will disappear altogether in the future. In contrast, no significant changes are predicted in AN blocking frequency and duration.

[20] Wintertime westerlies around south-east Australia and New Zealand are strongly dependent on the horizontal resolution of the AGCM: the lower the horizontal resolution is, the less remarkable the split over New Zealand is. Since state-of-the-art climate models discussed in the IPCC-AR4 report have spatial resolutions of a hundred kilometers or so, introducing higher models can lead to a reduction of uncertainties in the projections of future climate around south-east Australia and New Zealand.

[21] **Acknowledgments.** This work was performed under the framework of the project “Projection of the Change in Future Weather Extremes using Super-High-Resolution Atmospheric Models” supported by the KAKUSHIN Program of the Ministry of Education, Culture, Sports, Science and Technology (MEXT) of Japan. The calculations were performed using the Earth Simulator.

## References

- Archer, C. L., and K. Caldeira (2008), Historical trends in the jet streams, *Geophys. Res. Lett.*, *35*, L08803, doi:10.1029/2008GL033614.
- Bals-Elsholz, T. M., E. H. Atallah, L. F. Bosart, T. A. Wasula, M. J. Cempa, and A. R. Lupo (2001), The wintertime Southern Hemisphere split jet: Structure, variability, and evolution, *J. Clim.*, *14*, 4191–4215.
- Cash, B. A., and S. Lee (2000), Dynamical processes of block evolution, *J. Atmos. Sci.*, *57*, 3202–3218.
- D’Andrea, F., et al. (1998), Northern Hemisphere atmospheric blocking as simulated by 15 atmospheric general circulation models in the period 1979–1988, *Clim. Dyn.*, *14*, 385–407.
- Inatsu, M., and B. J. Hoskins (2004), The zonal asymmetry of the Southern Hemisphere winter storm track, *J. Clim.*, *17*, 4882–4892.
- Intergovernmental Panel on Climate Change (2007), *Climate Change 2007: The Physical Science Basis—Contribution of Working Group I to the Fourth Assessment Report of the Intergovernmental Panel on Climate Change*, edited by S. Solomon et al., Cambridge Univ. Press, New York.
- Matsueda, M., R. Mizuta, and S. Kusunoki (2009), Future change in wintertime atmospheric blocking simulated using a 20-km-mesh atmospheric global circulation model, *J. Geophys. Res.*, *114*, D12114, doi:10.1029/2009JD011919.
- Mendes, M. C. D., R. M. Trigo, I. F. A. Cavalcanti, and C. C. DaCamara (2008), Blocking episodes in the Southern Hemisphere: Impact on the climate of adjacent continental areas, *Pure Appl. Geophys.*, *165*, 1941–1962.
- Mizuta, R., et al. (2006), 20-km-mesh global climate simulations using JMA-GSM model—mean climate states—, *J. Meteorol. Soc. Jpn.*, *84*, 165–185.
- Mizuta, R., Y. Adachi, S. Yukimoto, and S. Kusunoki (2008), Estimation of future distribution of sea surface temperature and sea ice using CMIP3 multi-model ensemble mean, *Tech. Rep. MRI 56*, Meteorol. Res. Inst., Tsukuba, Japan.
- Onogi, K., et al. (2007), The JRA-25 reanalysis, *J. Meteorol. Soc. Jpn.*, *85*, 369–432.
- Palmer, T. N., F. J. Doblas-Reyes, A. Weisheimer, and M. J. Rodwell (2008), Toward seamless prediction: Calibration of climate change projections using seasonal forecasts, *Bull. Am. Meteorol. Soc.*, *89*, 459–470.

- Tibaldi, S., E. Tosi, A. Navarra, and L. Pedulli (1994), Northern and Southern hemisphere seasonal variability of blocking frequency and predictability, *Mon. Weather Rev.*, *122*, 1971–2003.
- Trenberth, K. E. (1979), Interannual variability of the 500 mb zonal mean flow in the Southern Hemisphere, *Mon. Weather Rev.*, *107*, 1515–1524.
- Trenberth, K. E., and K. C. Mo (1985), Blocking in the Southern Hemisphere, *Mon. Weather Rev.*, *113*, 3–21.
- Trigo, R. M., I. F. Trigo, C. C. DaCamara, and T. J. Osborn (2004), Climate impact of the European winter blocking episodes from the NCEP/NCAR reanalyses, *Clim. Dyn.*, *23*, 17–28.
- 
- H. Endo and R. Mizuta, Climate Research Department, Meteorological Research Institute, 1-1, Nagamine, Tsukuba, Ibaraki 305-0052, Japan.
- M. Matsueda, Advanced Earth Science and Technology Organization, Meteorological Research Institute, 1-1, Nagamine, Tsukuba, Ibaraki 305-0052, Japan. (mimatsue@mri-jma.go.jp)